S 08050
P.34

GROUND DEVELOPMENT AND FLIGHT CORRELATION OF THE VORTEX ATTENUATING SPLINE DEVICE

James C. Patterson, Jr., Earl C. Hastings, Jr.,
and Frank L. Jordan, Jr.

NASA Langley Research Center

SUMMARY

The data presented in this report indicate that the wing-mounted spline is a effective vortex-attenuating device. A comparison of the vortex-induced rolling moment results at a separation scale distance of 0.70 km (0.38 n. mi,) obtained in the Langley Vortex Research Facility with those measured in full-scale flight indicate good agreement for the unattenuated vortex configuration. The comparison also indicates that the spline effectiveness in flight was greater than in the ground facility test. The results of an applications study show that, for the heavy commercial jet aircraft studied, use of the splines does result in some degradation of the climb gradient and rate of climb, but the aircraft should meet certification requirements.

INTRODUCTION

The introduction of large, wide-body transport aircraft has resulted in an additional safety problem in the terminal area because of the strength and persistence of the lift-induced vortex. Because vortex strength is a

function of the lift for a particular aspect ratio and wing platform, the vortexes produced by the heavy transport aircraft that are now in service have become a hazard to following aircraft. The persistent nature of the vortex flow prolongs this unseen hazard to long after the vortex-generating aircraft has passed. NASA is engaged in a broad research program to increase understanding of vortex behavior and to develop methods of attenuating the trailing vortexes.

This paper presents the results of some of the experimental research and development at Langley Research Center of a vortex-attenuating device referred to as a spline. The areas of research discussed include the development of the spline device in the Langley Vortex Research Facility, a correlation of full-scale and small-scale test results, and results of an applications study to evaluate the impact of employing splines on a modern, heavy jet transport aircraft.

SYMBOLS

b wing span, m

$\bar{c}$ mean geometric chord, m

C_{ℓ_p} rolling moment due to rolling velocity, $\partial C_\ell/\partial(pb/2U)$ per rad

C_{ℓ_r} rolling moment due to yawing velocity, $\partial C_\ell/\partial(rb/2U)$ per rad

C_{ℓ_v} vortex-induced rolling-moment coefficient

C_{ℓ_β} rolling moment due to sideslip, $\partial C_\ell/\partial\beta$ per rad

$C_{\ell_{\delta_a}}$ rolling moment due to total aileron deflection, $\partial C_\ell/\partial\delta_a$ per rad

$C_{\ell_{\delta_r}}$ rolling moment due to rudder deflection, $\partial C_\ell/\partial \delta_r$ per rad

I_{xx} moment of inertia about longitudinal body axis, kg-m^2

I_{YY} moment of inertia about lateral body axis, kg-m^2

I_{zz} moment of inertia about vertical body axis, kg-m^2

J_{xz} roll-yaw product of inertia, kg-m^2

L rolling moment, m-N

p angular rate about longitudinal body axis, rad/s

q dynamic pressure, N/m^2

q' angular rate about lateral body axis, rad/s

r angular rate about vertical body axis, rad/s

S wing area, m^2

U velocity component along the longitudinal body axis, m/s

β angle of sideslip, rad

δ_a total aileron deflection, rad

δ_r rudder deflection, rad

θ pitch attitude in Earth reference system, rad

ϕ roll attitude in Earth reference system, rad

ψ heading relative to Earth reference system, rad

TESTS IN THE LANGLEY VORTEX RESEARCH FACILITY

Preliminary Vortex Research

Early vortex research that led to the spline concept was conducted in a pilot version of the Langley Vortex Research Facility. This pilot facility used a stationary airflow visualization method allowing a greater insight

into the actual motions of the wingtip vortex. The flow visualization method (ref. 1) developed in the pilot Vortex Research Facility is based on the fact that the air molecules affected by the wingtip are set into circular motion with no longitudinal flaw, with the exception of those molecules in the vortex core itself. To make this circular vortex motion visible, a screen of smoke is produced through which a model is propelled. As the model passes through the smoke screen, and for some time afterward, it is possible to photograph the entire life span of the vortex. (Although this same relative motion is present in the conventional wind tunnel, the test section usually is not of sufficient length to observe the full development of the vortex.

The first tests were conducted using a wing panel mounted on the monorail catapult system in the Langley towing basin. Preliminary runs were made that illustrated the vortex-alleviating effect of a number of configurations. These configurations were essentially geometric modifications of the wingtip, such as end plates, tip planform variations, tip extensions, flow-through nacelles, and many others that had only a small effect on the far-field vortex flow, and were, therefore, not solutions to the vortex persistence problem.

It was proposed that an unfavorable or positive pressure gradient applied just downstream of the wingtip might force the vortex to dissipate. This pressure gradient was applied by a decelerating chute at each wingtip, which virtually eliminated the vortex flow in both the near and far field. The mechanism behind the success of this approach is believed to be the result of disrupting the vortex axial flow plus the shearing stress between the rotational vortex flow and the linear flow of the mass of air forced forward into

each vortex core by the decelerating chutes. As a more practical application of this idea, the spline concept was tested and found to produce the same vortex attenuating effect as the decelerating chute. The spline configuration has the advantage that it can be readily retracted during cruise flight and deployed for landing.

Langley Vortex Research Facility Description

The later small-scale, spline vortex attenuation tests described in this paper were conducted in the Vortex Research Facility. In this new facility the stationary airflow visualization method was again employed as in the earlier investigations. It was possible to determine the aerodynamic forces associated with the vortex generating model, and by positioning a second model in this vortex core downstream of the lead model it was possible to determine the vortex-induced rolling moment. An overall view of the Vortex Research Facility is shown in figure 1. The carriage is mounted on the 548.64-m overhead track, with a vortex-generating aircraft model blade mounted beneath this carriage, and a following vortex probe model located 48.77 m downstream (a scale distance of 0.70 km), through a series of trailers to measure the induced rolling moment resulting from the lead model vortex.

The test section, constructed to isolate the wake of the carriage and trailers from the model wake, is 91.4 m long with a 5.08-cm opening along the center of the ceiling to allow the model blade mounts to pass. The exterior of the building shown at the entrance of the test section encloses the entire length of the track.

Test Model Description

Photographs of the two models used in the spline vortex attenuation investigation are shown in figures 2 and 3. These are 0.07-scale models of the generating aircraft and probe aircraft used in the full-scale flight tests discussed later in this paper.

The model of the vortex generating aircraft with the spline device installed on the wingtip was blade mounted beneath the carriage on an internal six-component strain-gage balance. The three-bladed model propellers were free to rotate as the model moved through the test facility. The effect of thrust was determined by powering each model propeller with a small reciprocating engine capable of producing the scale thrust level of an engine on the full-scale generating aircraft, The effects of thrust were negligible.

The 0.07-scale model of the low wing, single engine vortex probe aircraft is shown in figure 3. At this scale, the mean geometric wing chord of this model is 11.43 cm, resulting in a Reynolds number of 230 000 at the test velocity of approximately 30.48 m/s. Although low Reynolds number lift data are not available for this type of aircraft, it was doubtful, based on the data from the low Reynolds number test of reference 2, that the flow over the model wing was attached at the angles of attack induced by the vortex. During early tests the roll measurements made were unusually constant throughout the length of the test section. The probe aircraft model was in one fixed position relative to the wingtip of the vortex generating model during each run, and as a result of the vortex meander, this model was not perfectly centered in the vortex at all times throughout the entire length of the test

section. The induced rolling moment measured by the probe model therefore varied with the degree of vortex penetration. The constant rolling moment measured, therefore, indicated that the wing of the probe model was, indeed, stalled and that the vortex-induced roll was probably greater than that measured at this low Reynolds number.

To avoid this reduced performance for the following model, the wing panels of the probe model were deflected in a manner to reduce the relative vortex-induced angle of attack. When penetration of the vortex produced by the left wing of the generating model occurs, an upflow is imposed on the left wing of the probe model and a downflow on the right wing. By reduction of the angle of attack of the left wing and increase of that of the right wing by physically deflecting each wing panel separately, the vortex tangential velocity relative to each wing panel is reduced, such that the induced angle of attack is below the angle at which wing stall occurs at the test Reynolds number. The wing panel deflection angle resulting in the greatest measured vortex induced-rolling moment was found to be $\pm 3^{\circ}$.

Transition was fixed by applying a 100-grit Carborundum strip of 0.254 cm width on all upper and lower surfaces at the 5-percent local chord position.

TEST RESULTS

Effect of Spline Spanwise-Position

The formation of the lift-induced vortex occurs near the tip of a lifting wing having a constant span load over a large percent of the span,

such as that theoretically associated with a wing that is not tapered, twisted, or swept. The wing of the generating model used in this investigation was tapered and twisted; therefore, the final rollup of all the small vortexes formed along the span of the wing with each change in lift, plus the vortex created at the wingtip, coalesce inboard of the wing tip. Model tests were conducted to determine this rollup position, using the flow visualization technique of reference 1. The spline device was positioned at this location and at other spanwise locations along the wing span while the resulting rolling moment was measured by the probe model to determine the spanwise position that produces the maximum vortex alleviation. These rolling moment values induced on the probe model at a separation distance of 0.23 km are presented in figure 4.

The basic data of figure 4 show the maximum rolling moment induced by the generating model without vortex attenuation. The reduction in vortex-induced rolling moment attributed to the wingtip-mounted spline device is approximately 28 percent of the maximum. The attenuating effect becomes progressively greater as the spline is moved inboard, reaching a maximum roll reduction at approximately the 75-percent semispan position. The induced rolling moment at this point is reduced approximately 36 percent below that for the configuration without splines. These force data also indicate that the attenuating effect of the spline decreases as the spline is moved further inboard. The spline was tip mounted for the full-scale flight test because of structural considerations; therefore, the flight rolling-moment measurements presented here are considered somewhat conservative.

Visual data for the unattenuated configuration presented on figure 5 indicate the formation of the vortex system as this model moves through the smoke screen. The distinct vortex cores, the surrounding circulatory field, and the wing downwash may readily be seen as well as the growth and movement of the vortex system with time. The final photograph is of the probe model as it penetrates the vortex produced by the left wing panel of the generating model.

Visual data obtained for the generating model with tipmounted splines presented in figure 6 indicate that the high-energy vortex core produced by the basic unattenuated model is eliminated by the flow field of the spline device and the circulation around the core is greatly reduced. The vortex probe model shown in the final photograph measures the rolling moment induced by this altered vortex. Visual data obtained with the spline device located at the various spanwise positions (not shown) indicate a more dispersed flow pattern than shown here. As the splines are moved inboard along the span there is a tendency for the tip vortex to form, but it is rapidly dissipated as it moves into the flow field produced by the spline.

Visual data of the wake at separation distances several kilometers (miles) downstream from the vortex generating model indicate that there is a tendency for the vortex to reform possibly as a result of the remaining circulation. This same result was also noted during flight test, although the large diameter vortex that did reform when penetrated by the probe aircraft induced very little roll.

Effect of Spline Diameter

Preliminary qualitative results obtained in the pilot facility (ref. 1) indicate that the required spline diameter for vortex attenuation below the hazard level was approximately 55 percent of the wing mean geometric chord. The effect of spline diameter on the vortex-induced rolling moment measured in the Vortex Research Facility by the following model is presented in figure 7. These data indicate that the vortex attenuation of the spline device is a function of the exposed area as would be expected. However, reducing the diameter from 55 to 35 percent $\bar{c}$ resulted in only a small change in the reduction in induced rolling moment. Wind tunnel tests have shown that the drag associated with the spline is a direct function of frontal area, therefore, the 35-percent diameter spline would have substantially less drag than the 55-percent diameter spline. Therefore, the 40-percent-diameter spline would probably be optimum, considering both vortex attenuation and drag. The smallest diameter spline tested (27 percent $\bar{c}$) resulted in a sizable decrease in vortex attenuation while the largest spline tested (65 percent $\bar{c}$) resulted in an increase in vortex attenuation that extended much farther downstream and prevented the vortex from reforming. However, it would be expected that this larger spline would cause significant increase in drag.

The effect of spline diameter on the development of the lift-induced vortex is shown visually on figure 8. These data were obtained approximately 0.23 km (0.13 n. mi.) downstream from the vortex generating model. The results for the smallest diameter spline (upper left-hand photograph) indicate the vortex is beginning to reform at this short separation distance. As the

spline diamater is increased, it can be seen that vortex development is further retarded.

Effect of Spline Chordwise Position

The spline position behind the wing trailing edge was based on experimental wind tunnel tests (not reported) such that the impingement of the spline pressure field on the wing surfaces causes a minimum loss in lift and increase in drag. The increase in drag during landing is not considered as significant as any loss of lift might be.

FLIGHT TEST DESCRIPTION

Detailed descriptions of the aircraft, systems, and procedures used in these tests are presented in reference 3 and summarized briefly here.

The aircraft shown in figure 9 was used as the generating aircraft because it was available and could be adapted for tip splines without undue time or expense. Some additional characteristics of the generating aircraft used are as follows:

Empty operational mass, kg (lb_m)	22 294 (49 150)
Wing area, m^2 (ft^2)	135.8 (1462.0)
Wing mean aerodynamic chord, m (ft)	4 (13.61)
Wing aspect ratio	9.44
Wing incidence (root), deg	4
Wing incidence (tip) deg	1

Horizontal tail area, m^2 (ft^2) 30.2 (324.9)

Vertical tail area, m^2 (ft^2) . . . . . 16.7 (179'.3)

Engine . . . . . Pratt and Whitney 2000 D-5

Propeller data:

Type . . . . . Hamilton standard constant speed

Gear ratio. 2:1

Blade activity factor 100

Diameter, m (ft) 3.97 (13.0)

For these tests, the basic aircraft was modified by the installation of the splines (see fig. 10), a spline jettison system, and a flow visualization system for vortex marking. As previously noted, tests in the Vortex Research Facility indicated that splines located inboard of the wing tips would be more effective than splines located at the tips. (See fig. 4.) With flaps down, the optimum spline location would have been further inboard. However, because the extensive structural modifications required to locate the splines inboard precluded anything but a tip-mounted location, the flight tests were made with the splines at the wing tips and with the flaps retracted. Inflight motion pictures showed that this configuration positioned the splines in a location to interact with the tip vortexes, even though optimization of the spline location was not possible.

A diagram of the probe aircraft is shown in figure 11. For these tests, the probe aircraft was equipped with onboard distance measuring equipment (DME); an S-band radar tracking beacon, and a fixed 16-mm motion picture camera. Additional information on the characteristics of the probe aircraft

include the following:

Mass:

Empty operation, kg (lb_m)	799	(1761)
Gross takeoff, kg (lb_m)	1009	(2225)

Inertias (approximate):

I_{xx}, kg-m^2 (slug-ft^2)	1356	(1000)
I_{yy}, kg-m^2 (slug-ft^2)	1900	(1401)
I_{zz}, kg-m^2 (slug-ft^2)	2700	(1991)
J_{xz}, kg-m^2 (slug-ft^2)	67.6	(50)

Wing data:

Area, m^2 (ft^2)	14.9	(160)
Span, m (ft)	9.14	(30)
Chord, m (ft)	1.6	(5.3)

Aileron data:

Span, m (ft)	1.6	(5.3)
Chord, m (ft)	0.305	(1.0)

Engine type . . . . . Lycoming 0-360-A3A

On a typical penetration flight, the two aircraft would rendezvous and establish the desired airspeeds, headings, and altitudes. The probe aircraft records, DME, and camera were turned on, and the vortex-marking system in the generating aircraft was activated, When the desired separation distance between the two aircraft was established, the probe aircraft approached the vortex trail along a parallel course. Shallow-angle penetrations were then made from just above or below the trail. For flights without splines, penetrations were made at separation distances between 9.26 km (5 n. mi.) and

3.70 km (2 n. mi.). With splines installed, penetrations were made as close as 0.6 km (0.32 n. mi.). All penetrations were made in the flaps-up configuration at a nominal altitude of 2100 m (7000 ft) and indicated airspeeds of 50±5 m/s (90±10 knots). The test Reynolds number, based on these nominal values and the $\bar{c}$ of the probe aircraft, was 4.364×10^6.

In comparing vortex attenuation results from flight tests with those from ground facilities, a difference in testing technique should be noted. In these flight tests (as in flight tests in general) it was often difficult to precisely position the probe aircraft in the vortex core. Some factors that contributed to this difficulty were small vortex core, meander of the vortex because of atmospheric disturbances, and the tendency of the probe aircraft to roll away from the core. (In these tests, this problem was less severe with the attenuated (splines-deployed) vortex because the core size was larger and the vortex less intense.) Data presented from the Vortex Research Facility, however, were determined when it was certain that the probe model was within the vortex core.

To minimize this difference in test technique, the flight tests involved a large number of penetrations to increase the probability that the maximum possible induced-roll accelerations of the probe aircraft were achieved. The validity of this technique is discussed later in this paper.

DATA ANALYSIS AND RESULTS

One of the parameters used to evaluate vortex attenuation effectiveness was the maximum roll acceleration $\dot{p}_{max}$ derived from measured rate data recorded

by the probe aircraft during penetrations with controls as nearly neutral as possible. Many penetrations were made to provide a large statistical sampling. The maximum values obtained (ref. 3) are shown in figure 12. Data are presented for the generating aircraft without splines, and with the 2.28-m splines installed. It is evident that the splines were effective in attenuating the vortex effects over the range of distances shown.

As noted in reference 3, these results include the effects of small aileron deflections. To provide a comparison of the flight data with data from the Vortex Research Facility, additional analyses were conducted to express the flight results in terms of the rolling-moment coefficient resulting from vortex alone.

The equation of motion in roll (see ref. 4, ch. 3) is given by

$$L = \dot{p}I_{xx} - \dot{r}J_{xz} + q'r(I_{zz} - I_{yy}) - pqJ_{xz} \tag{1}$$

where a dot above a symbol denotes a derivative with respect to time.

The linearized equation, expressed in terms of rolling-moment coefficients (ref. 4), is

$$\frac{I_{xx}\ddot{\phi}}{qSb} - \frac{J_{xz}\ddot{\psi}}{qSb} - \frac{\dot{\phi}b}{2U} C_{\ell_1} - \frac{\dot{\psi}b}{2U} C_{\ell_r} - C_{\ell_\beta}\beta = C_{\ell_{\delta_a}}\delta_a + C_{\ell_{\delta_r}}\delta_r \tag{2}$$

where

$$\dot{\phi} = p + q' \sin\phi \tan\theta + r \cos\phi \tan\theta \tag{3}$$

and

$$\psi = (q' \sin \phi + r \cos \phi) \sec \theta \tag{4}$$

Equation (2) was used as the basis of this analysis because a computer program was available and sample cases showed less than a 4 percent difference in the results from the complete and linearized (computer) methods.

Adding a term C_{ℓ_V} for the vortex effect, and transposing terms in equation (2), gives the relationship used in this analysis:

$$C_{\ell_V} = \frac{I_{xx}\ddot{\phi}}{qSb} - \frac{J_{xz}\ddot{\psi}}{qSb} - \frac{\dot{\phi}b}{2U} C_{\ell_p} - \frac{\psi b}{2U} C_{\ell_r} - C_{\ell_\beta} B - C_{\ell_{\delta_a}} \delta_a - C_{\ell_{\delta_r}} \delta_r \tag{5}$$

Equation (5) was used to determine values of C_{ℓ_V} at 0.1-s time intervals during each vortex penetration of interest, and the maximum values are presented as the flight test C_{ℓ_V} values in this report. In the solution of equation (5), the inertias, wing area, and wing span of the probe aircraft were used. Aerodynamic and control derivatives were those obtained in earlier Langley Research Center flight test and simulator tests with this aircraft:

C_{ℓ_p}, rad^{-1}	-0.2741
C_{ℓ_r}, rad^{-1}	.07
C_{ℓ_β}, rad^{-1}	-.045
$C_{\ell_{\delta_a}}$, rad^{-1}	-.0365
$C_{\ell_{\delta_r}}$, rad^{-1}	-.014

Airspeed, dynamic pressure, control position, attitude, and rate information were determined from measurements recorded during the vortex penetrations.

An indication of the accuracy of this procedure was shown, using the results of flight tests with the probe aircraft in which aileron rolls were performed in undisturbed air ($C_{\ell_V} = 0$). Data as listed for probe aircraft and flight-test data were used with equation (5), and C_{ℓ_V} histories were calculated for a number of rollmaneuvers. In all cases, the maximum calculated values of C_{ℓ_V} were between 0 and 0.003. This indicated that the error resulting from the analytical method was much smaller than the vortex-induced values.

Maximum values of C_{R_V} from this analysis are shown in figure 13. The maximum aileron rolling moment coefficient, $C_{\ell_{\delta_a}} 6_{a_{max}}$ is also shown. The data show that for the unattenuated (no spline) vortex, the vortex-induced roll was larger than the maximum aileron roll at separation distances closer than 8 km (4 n. mi.) and was about 60 percent above that value at 4.11 km (2.22 n. mi.). For the attenuated (splines-on) case, the vortex-induced roll coefficient was always less than the roll capability of the aileron under the same conditions.

GROUND FACILITY/FLIGHT TEST CORRELATION

A comparison of the results obtained in the Langley Vortex Facility with those obtained in flight is presented in figure 14. The rolling moment induced by the lift-induced vortex of the 0.07-scale generating model was measured at a scale distance of 0.70 km (0.38 n. mi.) downstream of this model, although the flight data are presented at separation distances ranging

from 4.11 to 9.09 km. The flight data in this figure has been corrected to the same value of U/U_f (where U_f is the velocity of the following aircraft) as the 0.07 scale tests.

A flight rolling moment coefficient of the 0.058 is obtained for the basic configuration at a separation distance of 0.70 km using the straight line extrapolation shown. This extrapolation is based on flight test results presented by Marvin R. Barber, et al, in this report. There is reasonable agreement between the "no splines" data based on this extrapolation. This indicates that the test techniques employed in the ground and the flight experiments were valid for this configuration.

The attenuated rolling-moment coefficients (splines on) presented in figure 14 are for the wing-tip mounted spline device with a diameter equal to 55 percent of the mean geometric wing chord. It was possible during the flight test to probe as close as 0.60 km behind the vortex-generating aircraft allowing a direct comparison between flight and model test results.

The tip-mounted spline reduced the vortex-induced rolling moment in flight approximately 72 percent at a separation distance of 0.70 km while the model results indicate a vortex roll reduction of approximately 27 percent at this same separation distance. These data indicate that a greater vortex attenuating effect is derived from the spline device in flight than in the ground facility. Although the reason for this discrepancy has not yet been determined it might be conjectured then that Reynolds number may have a large affect on the flow field developed by the spline device reducing its vortex attenuating effect at model scale. The model visual data indicate that the well-organized vortex core is nearly eliminated while the circulation outside of the core remains and produces the rolling moment measured by the following model. The lower velocities associated with the circulation would be affected by model scale.

APPLICATIONS STUDY

During these flight tests, the performance of the generating aircraft with splines attached was evaluated and found to be acceptable (ref. 3). However, because this generating aircraft was not a representative commercial aircraft, a preliminary study was conducted for NASA by the Boeing Co. to evaluate the performance of the aircraft shown in figure 15. Results are presented in reference 5.

In summary, it was concluded that for splines deployed only on approach, the concept appears feasible from the standpoint of structures, stability and control, performance, and operations. The largest spline effects are decreases in landing climb gradient and climb rate, and an increase in approach noise. Even with these penalties, the aircraft would meet certification requirements. Effects on other parameters such as takeoff, cruise, range, approach speed, and so forth, were indicated to be insignificant.

CONCLUDING REMARKS

The results obtained during this investigation indicate that--

(1) The spline device is effective in reducing the strength of the lift-induced vortex.

(2) A comparison of the vortex-induced rolling moment obtained in the Langley Vortex Research Facility with full-scale flight results indicate good agreement for the unattenuated aircraft configuration. This implies that the test techniques employed on the ground and in flight experiments were valid.

(3) A comparison of data at 0.70 km indicates that the vortex attenuation achieved in flight was greater than was obtained in the ground facility, indicating that the ground facility was conservative with this device.

(4) A preliminary study indicated that the installation of splines on current commercial jet aircraft would be feasible. Significant penalties would result in the landing phase climb capability and approach noise. Even with the penalties, however, this aircraft would meet current certification requirements.

REFERENCES

1. Patterson, J. C., Jr.; and Jordan, F. L., Jr.: A Static-Air Flow Visualization Method to Obtain a Time History of the Lift-Induced Vortex and Circulation. NASA TM X-72769, 1975.
2. Jacobs, E. N.; and Sherman, A.: Airfoil Section Characteristics as Affected by Variation of Reynolds Number. NACA TR-586, 1937.
3. Hastings, E. C., Jr.; Patterson, J. C., Jr.; Shanks, R. E.; Champine, R. A.; Copeland, W. L.; and Young, D. C.: Development and Flight Tests of Vortex Attenuating Splines. NASA TN D-8083, 1975.
4. Blakelock, J. H.: Automatic Control of Aircraft and Missiles. John Wiley & Sons, Inc., Apr. 1965.
5. Tracey, P. W.; and Berger, John H.: The Effects of Installing Vortex Attenuation Devices on the Design, Performance, and Operations of a Heavy Commercial Jet Transport. Boeing Report Number D6-37174, 1975.

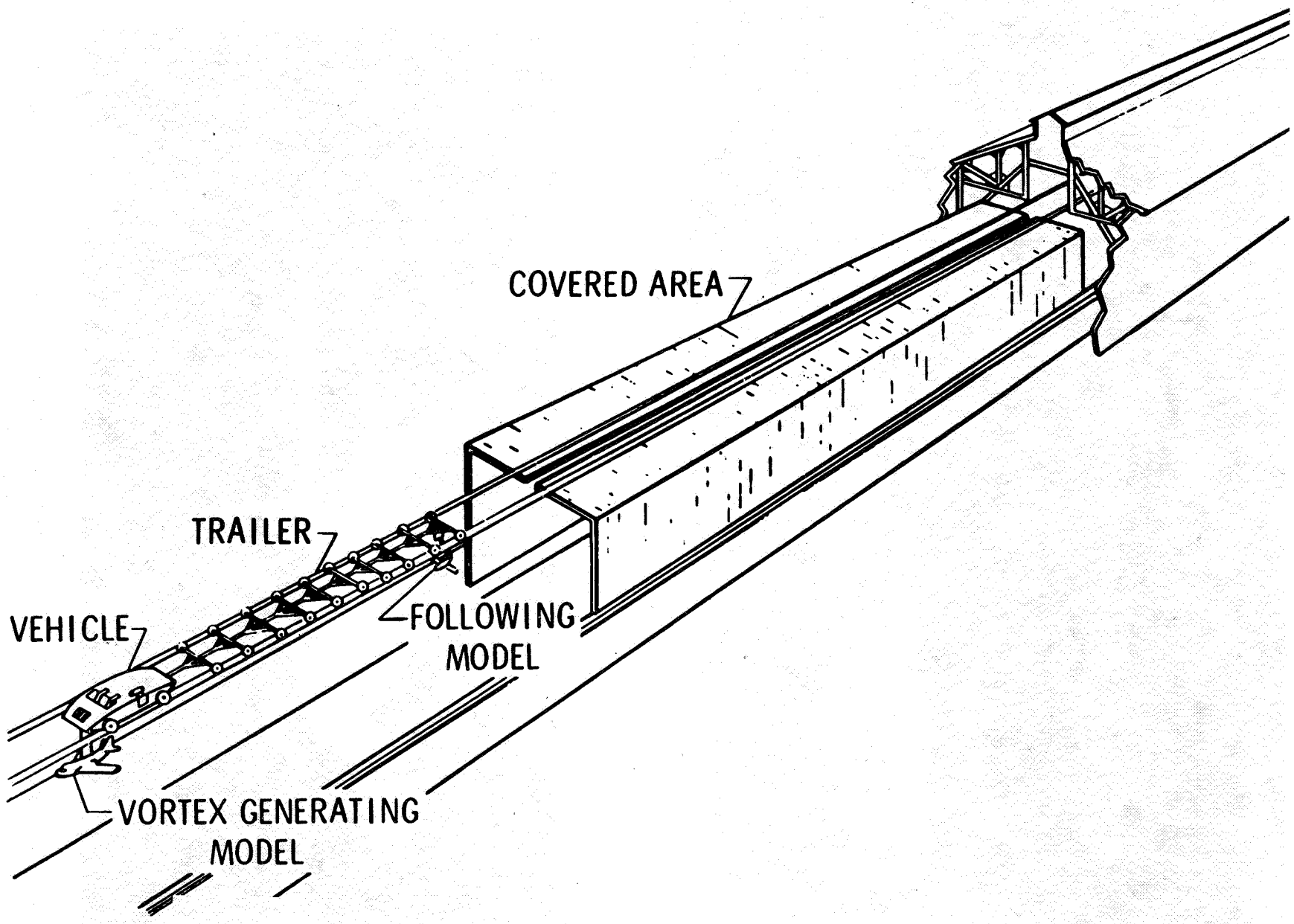

Figure 1.--Arrangement of the Langley Vortex Research Facility.

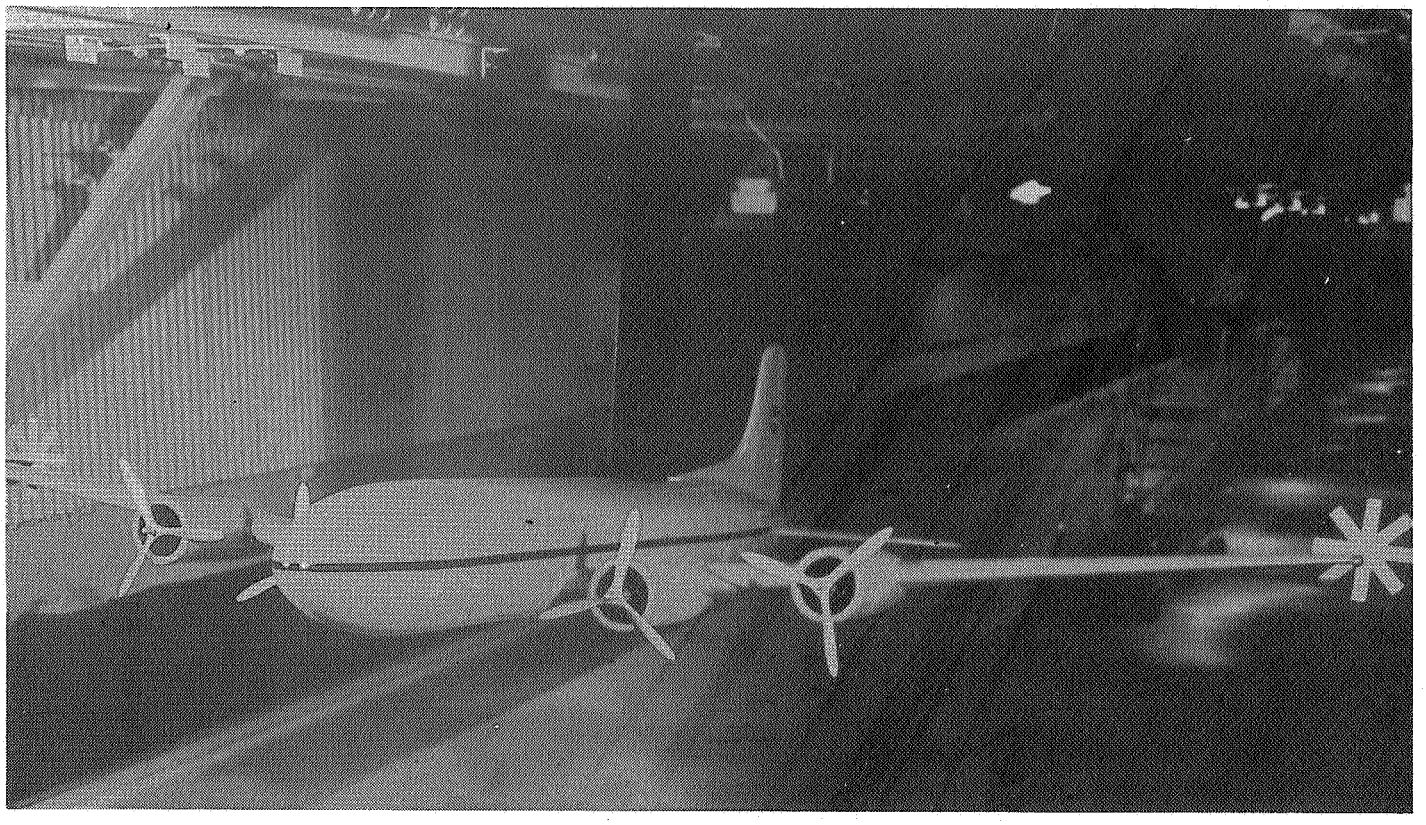

Figure 2.--Photograph of 0.07-scale model of propeller driven transport aircraft used as the vortex-generating model.

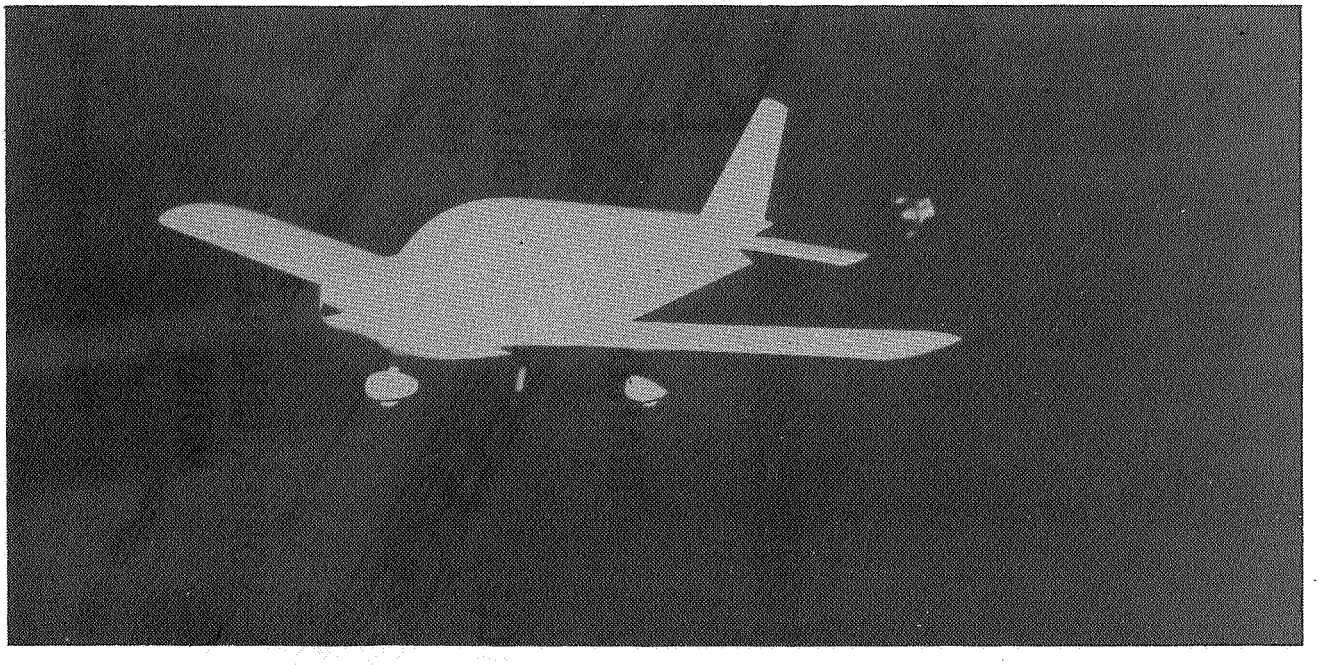

Figure 3.--Photograph of 0.07-scale model of single engine light aircraft used as the vortex probe model.

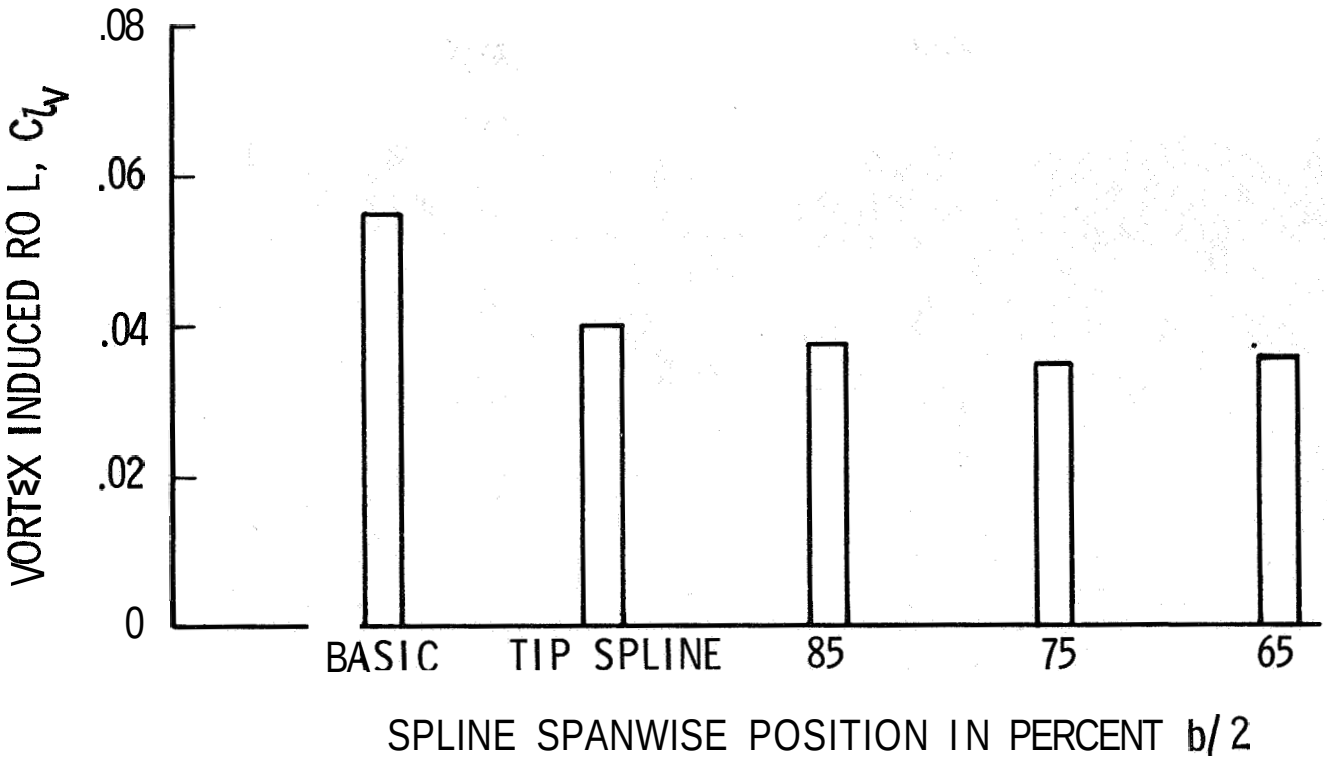

Figure 4.--Effect of spline spanwise position on vortex attenuation.

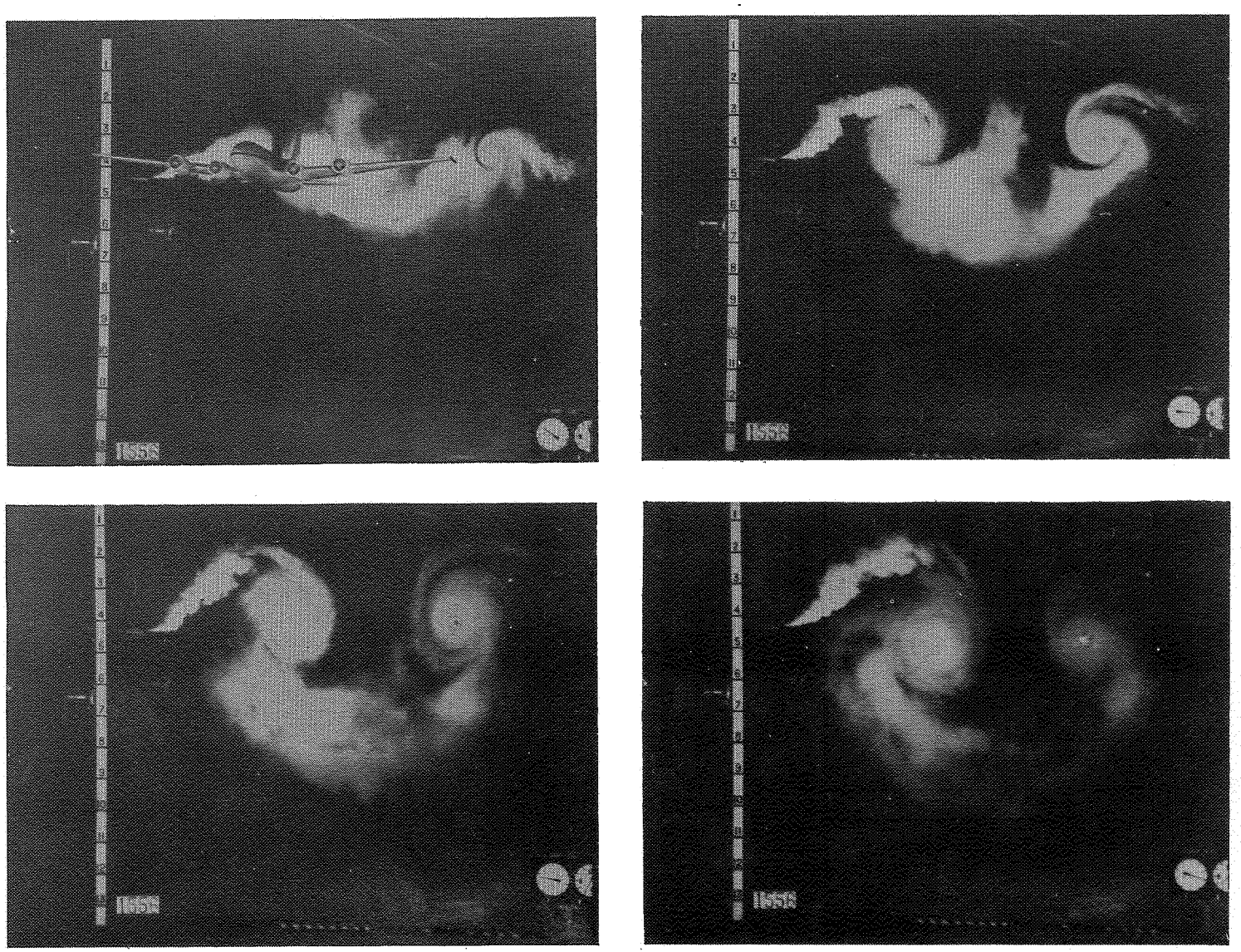

Figure 5 --Lift-induced vortex system created by 0.07-scale model of transport aircraft The photographic sequence rate corresponds to a separation distance of 0 23 km. The following model is centered in the vortex in the last photograph. Lift coefficient = 0 , velocity = 30.48 m/s.

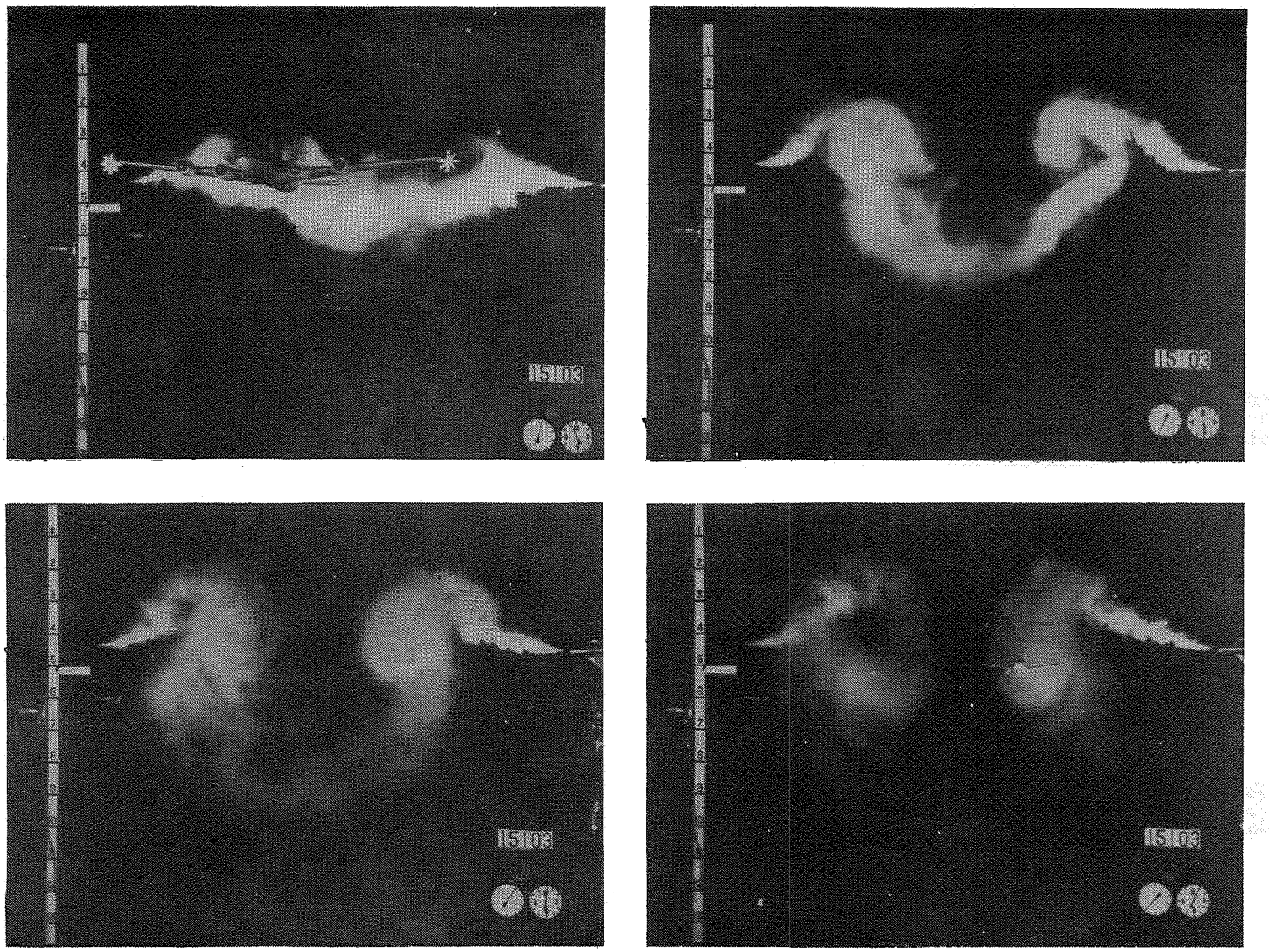

Figure 2 --Effect of the spline vortex attenuating device on the vortex system of transport aircraft The photographic sequence corresponds to a separation distance of 0 23 km. The following model is centered in the wortex in the last photograph. Lift coefficient = 0.8; velocity = 30 48 m/s

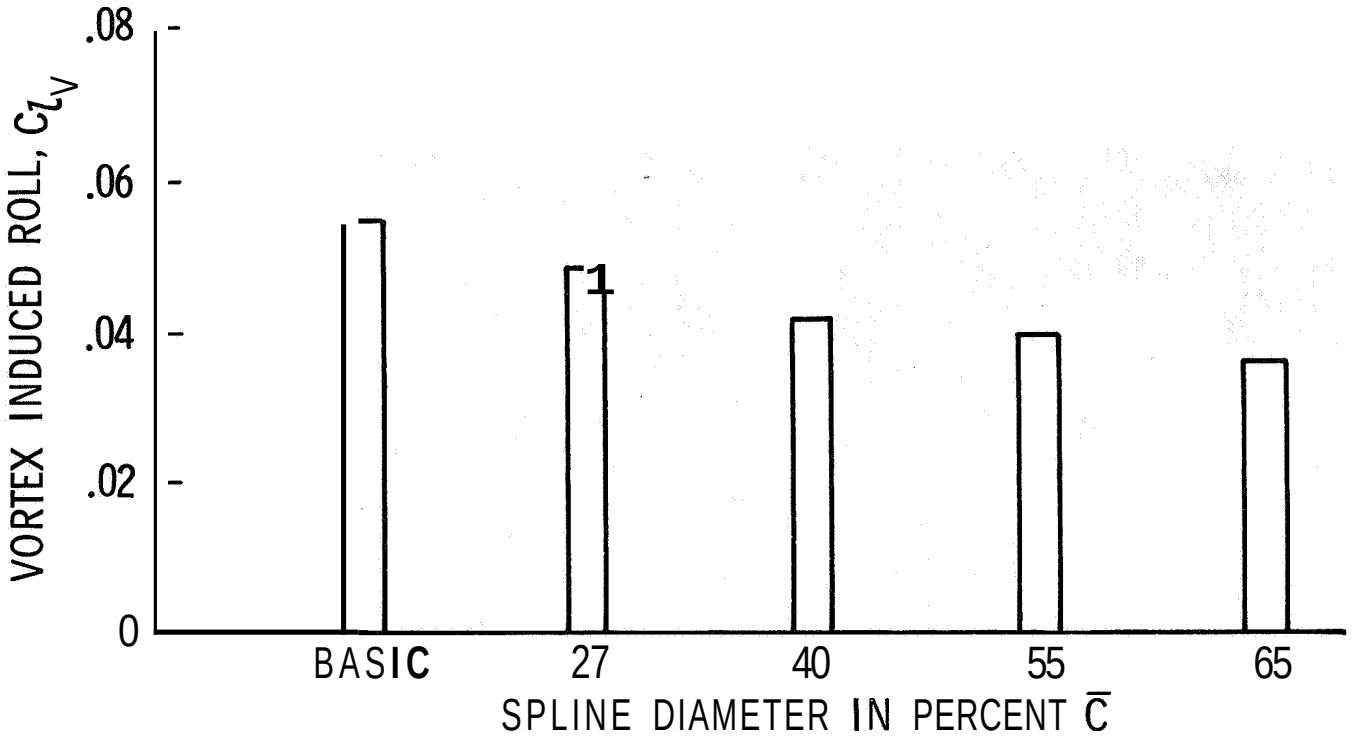

Figure 7.--Effect of spline diameter on the vortex attenuation of wingtip-mounted spline.

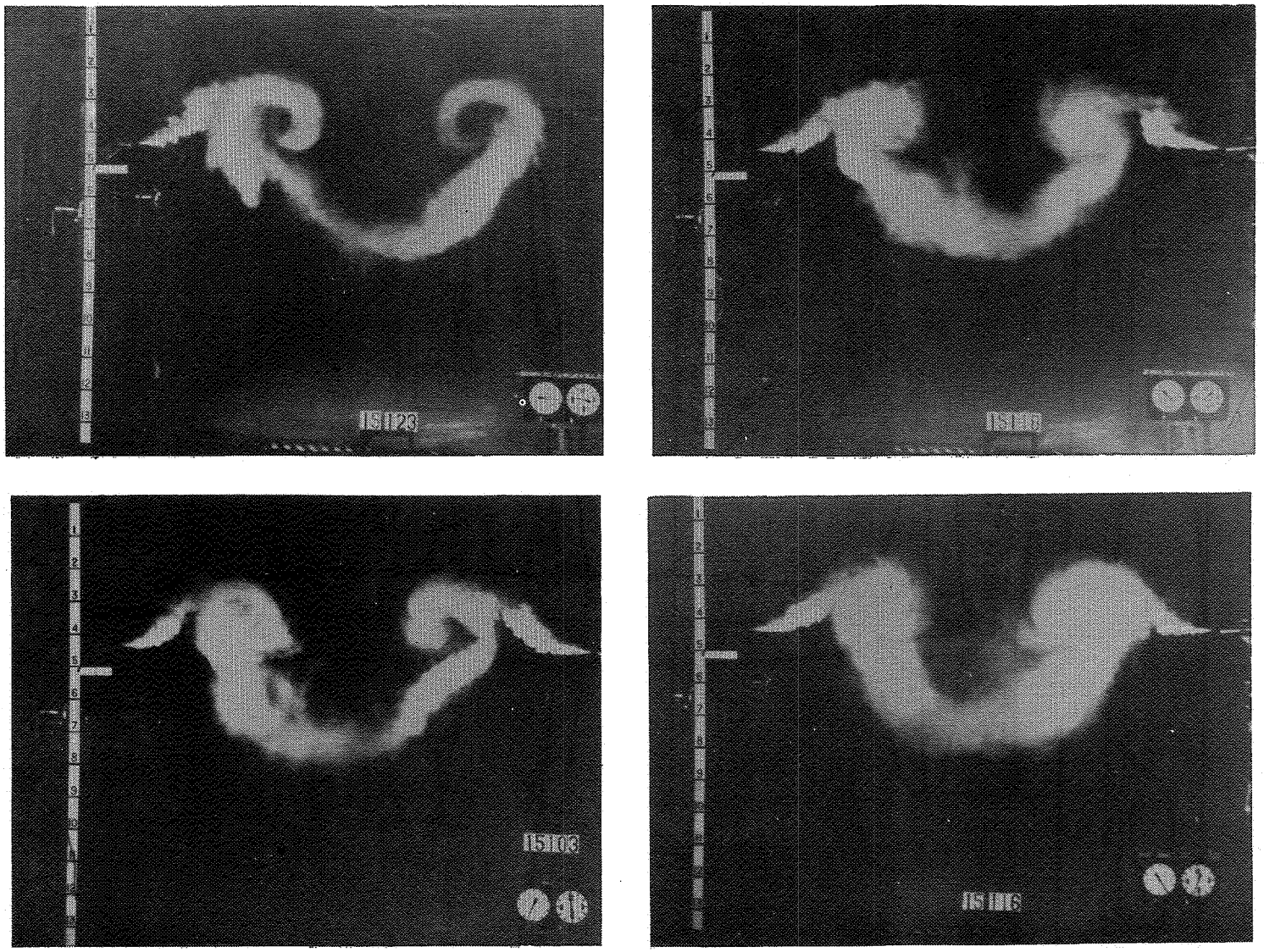

Figure 8 --Effect of spoiler diameter on vortex system from the transport aircraft at a separation distance of 0.23 km. Spoiler diameters at upper left are 25 percent of mean geometric chord; lower left, 50 percent; lower right, 60 percent.

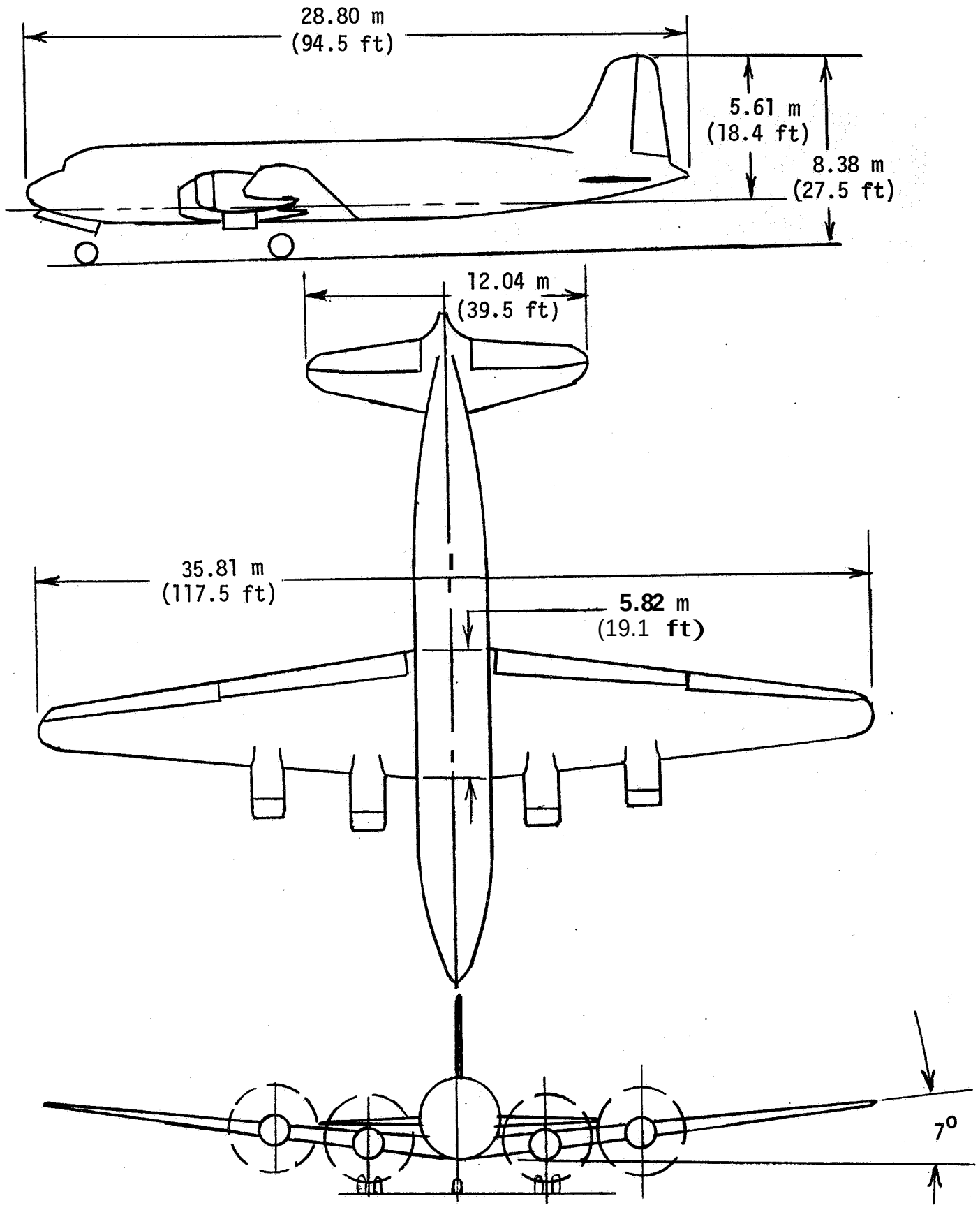

Figure 9.--Diagram of unmodified generating aircraft.

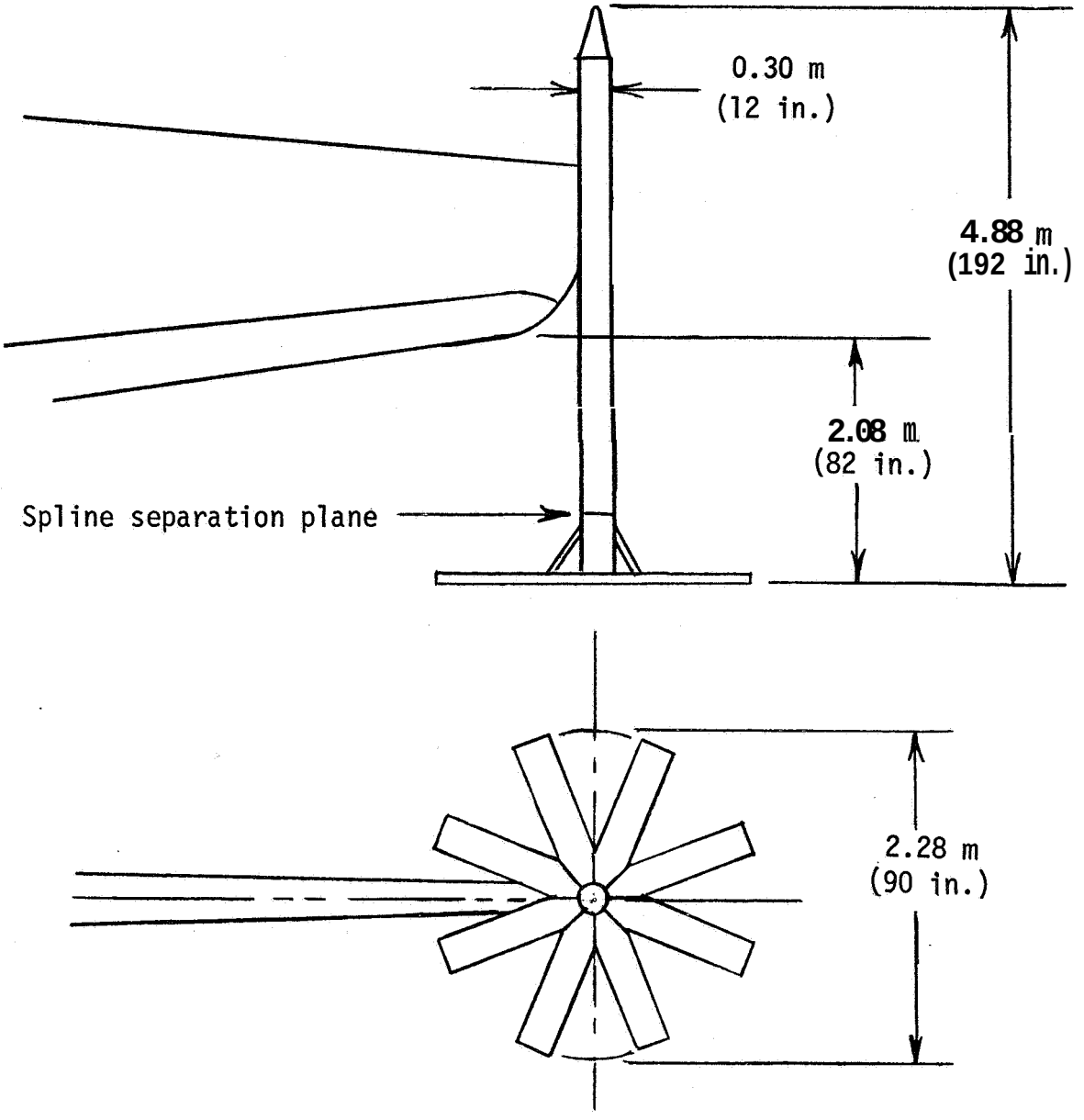

Figure 10.--Sketch of spline assembly at wingtip.

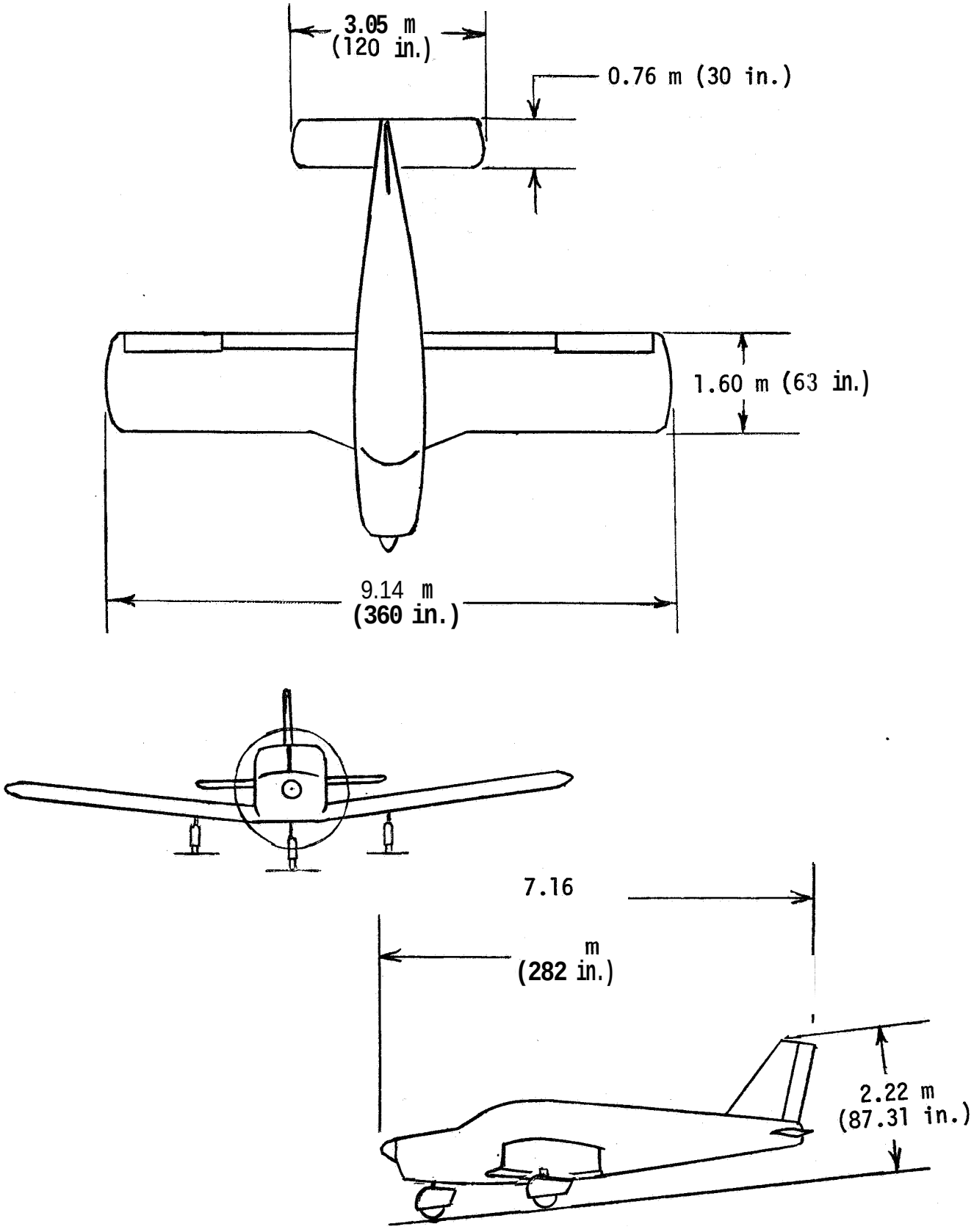

Figure 11.--Diagram of probe aircraft.

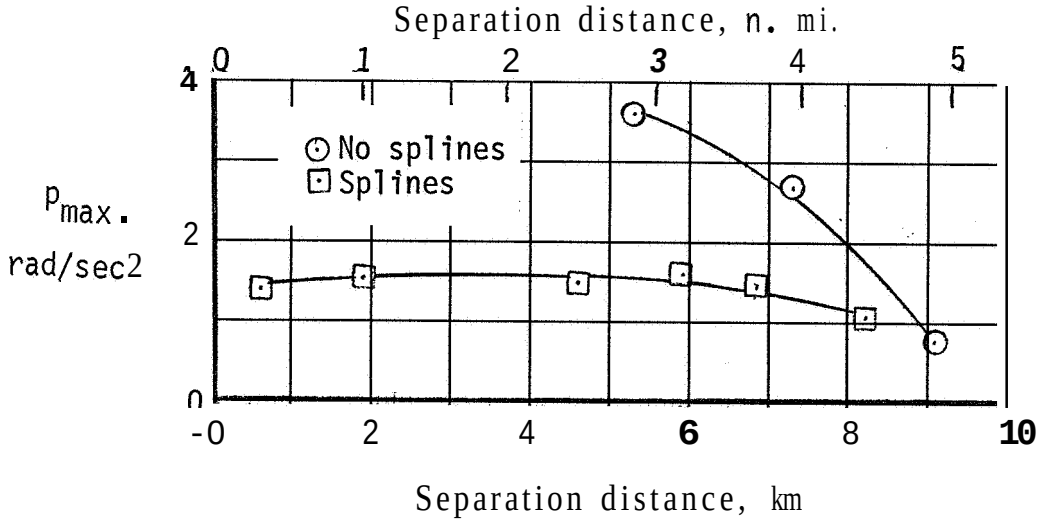

Figure 12.--Maximum roll acceleration.

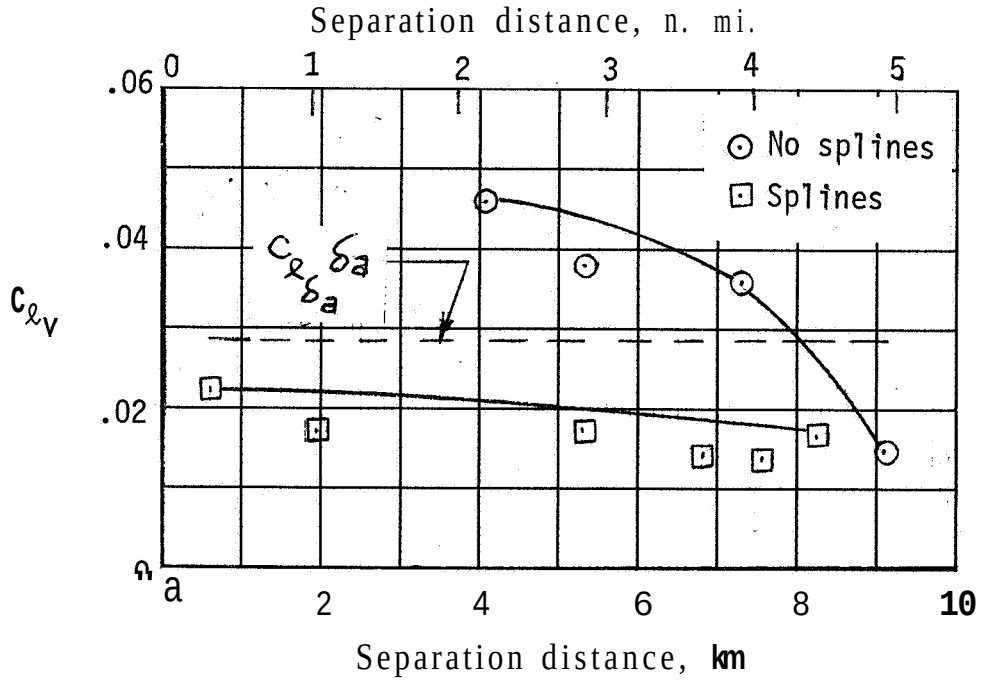

Figure 13.--Maximum vortex-induced rolling moment coefficient from flight tests.

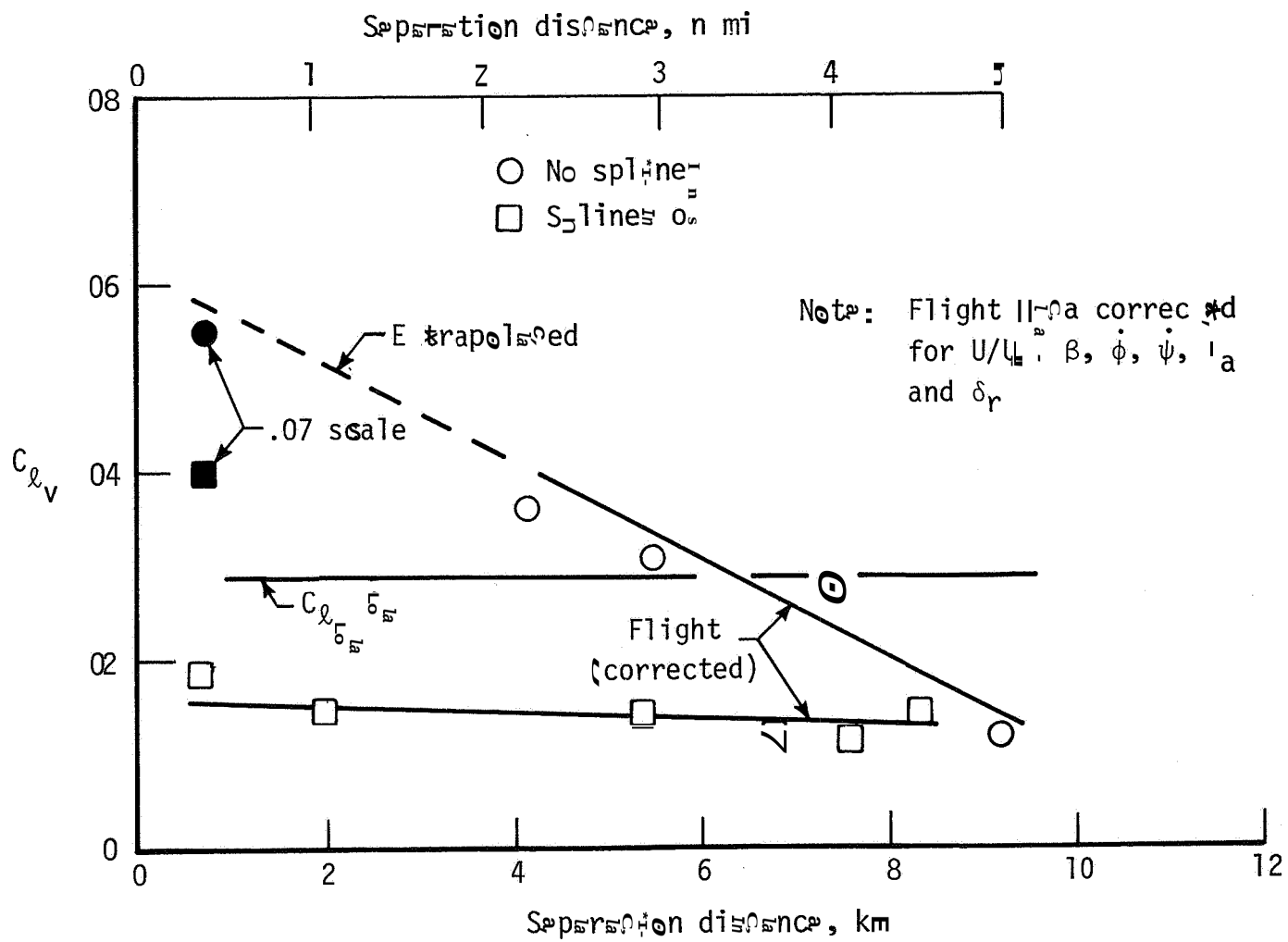

Figure 14 --Correlation of the vortex-induced rolling moment results obtained in flight and in the ground-based facility. Lift coefficient = 0.8.

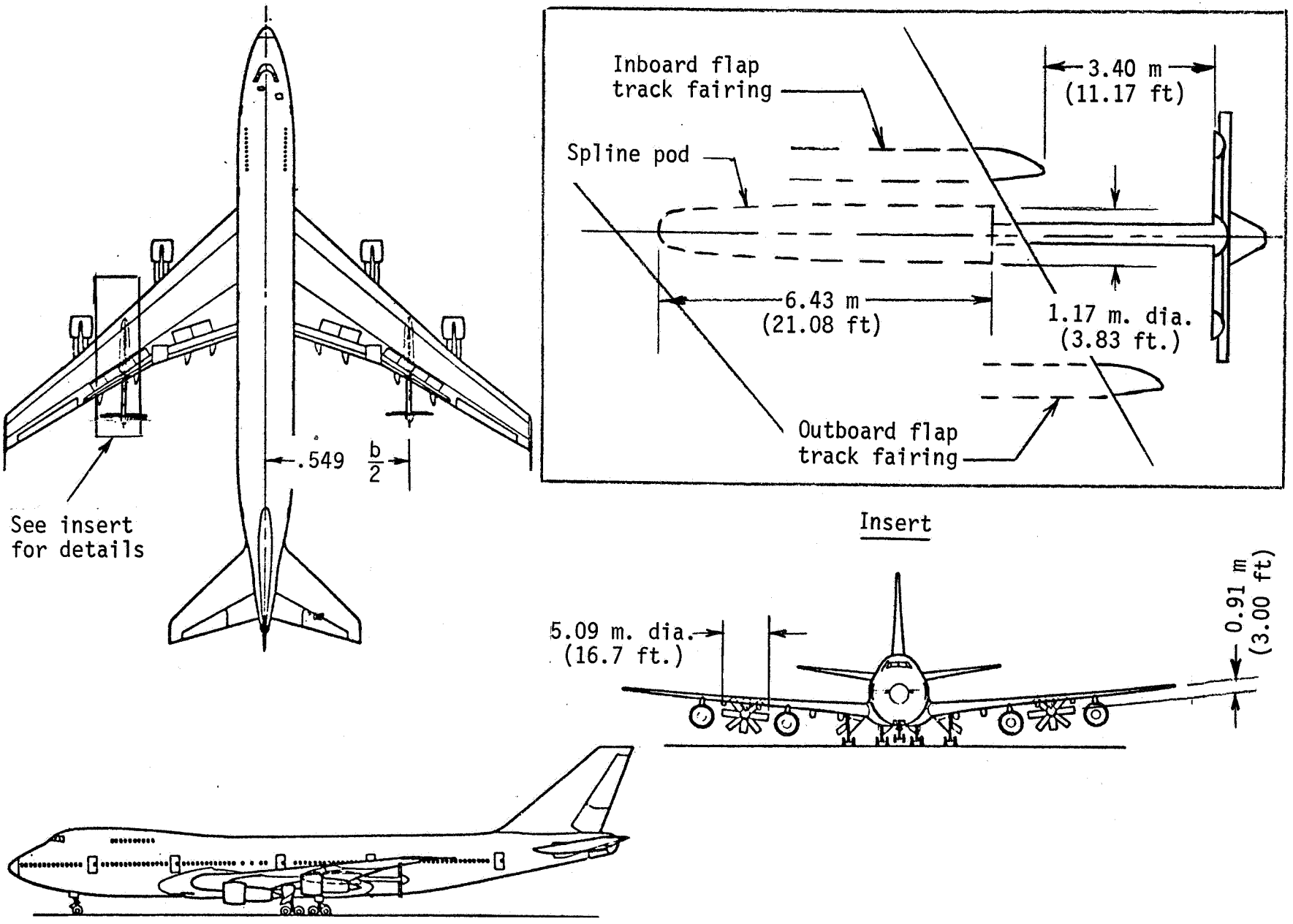

Figure 15.--Spline system installation on heavy commercial jet aircraft.